Bioresource Technology 418 (2025) 131991

Contents lists available at ScienceDirect

Bioresource Technology

journal homepage: www.elsevier.com/locate/biortech

Hydrazine promoted nitrite reduction in partial-denitrification by enhancing organic-substrate uptake and electron transport

Ben Dai [a,b], Jingzhou Zhou [a,b], Zuobin Wang [a,c], Yifeng Yang [d], Zhenyu Wang [a,b], Junxia He [a,b], Siqing Xia [a,b,*], Bruce E. Rittmann [e]

[a] State Key Laboratory of Pollution Control and Resource Reuse, College of Environmental Science and Engineering, Tongji University, Shanghai 200092, China
[b] Shanghai Institute of Pollution Control and Ecological Security, Shanghai 200092, China
[c] National Engineering Research Center of Dredging Technology and Equipment, Key Lab of Dredging Technology, CCCC, Shanghai, 200082, China
[d] Shanghai Municipal Engineering Design Institute (Group) Co., Ltd, Shanghai 200092, China
[e] Biodesign Swette Center for Environmental Biotechnology, Arizona State University, Tempe, AZ 85287-5701, United States

HIGHLIGHTS

- In the short term, N_2H_4 may interact with cytochrome *c* and inhibit NO_2^- reduction.
- However, long-term exposure to N_2H_4 led to more nitrite reduction.
- Long-term N_2H_4 exposure enriched the genera *OLB8*, *Thauera,* and *f_Rhodocyclaceae*.
- N_2H_4 promoted EPS formation, substrate uptake and utilization, electron transfer.
- Avoiding N_2H_4 release is vital for the success of partial denitrification-anammox.

GRAPHICAL ABSTRACT

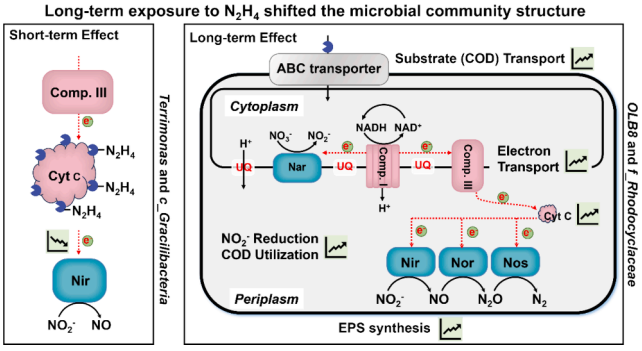

ARTICLE INFO

Keywords:
Denitratation
N_2H_4
Cytochrome *c*
Denitrification respiratory chain
Metagenomic analysis

ABSTRACT

Partial denitrification coupled with anammox is a promising approach for sustainable nitrogen removal from wastewater. However, this coupling can be influenced by hydrazine (N_2H_4) released by anammox bacteria. This study aimed to reveal how N_2H_4 regulates partial denitrification. Short-term batch experiments showed that 0.5 to 10 mg N/L of N_2H_4 promoted nitrite (NO_2^-) accumulation, likely by inhibiting the electron transfer from *cyt c* to nitrite reductase. However, long-term exposure to N_2H_4 (0.5 and 1 mg N/L) shifted the microbial community and increased NO_2^- reduction. This exposure enriched the genera *OLB8*, *Thauera*, and *f_Rhodocyclaceae*, and increased the abundance of genes involved in EPS formation, substrate transport and electron transport. The long-term outcome was more NO_2^- reduction to N_2 and more substrate (COD) oxidation. While N_2H_4 benefits NO_2^- accumulation in short-term, the mechanism is not sustainable, highlighting the importance of minimizing N_2H_4 release for successful in such coupled nitrogen removal systems.

* Corresponding author at: State Key Laboratory of Pollution Control and Resource Reuse, College of Environmental Science and Engineering, Tongji University, Shanghai 200092, China.
E-mail address: siqingxia@tongji.edu.cn (S. Xia).

https://doi.org/10.1016/j.biortech.2024.131991
Received 6 November 2024; Received in revised form 15 December 2024; Accepted 15 December 2024
Available online 16 December 2024
0960-8524/© 2024 Elsevier Ltd. All rights are reserved, including those for text and data mining, AI training, and similar technologies.

1. Introduction

Anammox has attracted significant attention as a potentially more sustainable and cost-effective method for nitrogen removal in wastewater treatment (Du et al., 2020). Anammox oxidizes ammonium (NH_4^+) into dinitrogen gas (N_2) using nitrite (NO_2^-) as the electron acceptor in anaerobic conditions (Kuypers et al., 2018):

$$NH_4^+ + 1.32NO_2^- + 0.066HCO_3^- + 0.13H^+ \rightarrow 1.02N_2 + 0.26NO_3^- + 0.066CH_2O_{0.5}N_{0.15} + 2.03H_2O$$

An intermediate in the anammox process is hydrazine (N_2H_4) (Ma et al., 2018; Zhang et al., 2024). Hydrazine is a highly reactive compound, and its very low redox potential ($E_0' = -750$ mV) makes it energy-rich and useful as rocket fuel (Dietl et al., 2015). Significant accumulation of N_2H_4 (up to 55 mg N_2H_4/L) has been observed in anammox processes (Ganesan and Vadivelu, 2019; Qiao et al., 2016; Sari et al., 2024), and the accumulation was influenced by factors such as organic matter, operating conditions, and heavy metals (Jin et al., 2012). The N_2H_4 released by anammox bacteria may have an impact on the partial nitrification and partial denitrification processes required to generate NO_2^- for anammox (Zhang et al., 2019; Z. Zhang et al., 2020).

For partial nitrification, N_2H_4 suppresses the activity of ammonium-oxidizing bacteria (AOB, oxidation of NH_4^+ to NO_2^-) and nitrite-oxidizing bacteria (NOB, oxidation of NO_2^- to NO_3^-) (Xiang and Gao, 2019). However, AOB are more tolerant of N_2H_4 than NOB, resulting in an increased proportion of AOB (Xiang and Gao, 2019; Zhang et al., 2022b). Therefore, the presence of N_2H_4 could promote the accumulation of NO_2^- in partial nitrification, similar to inhibition of NO_2^- oxidation by hydroxylamine (NH_2OH) (Terada et al., 2017; Zhao et al., 2021, 2022). The inhibition affects electron transport regulation, slows the activity of key catabolic enzymes, and alters the structure of the microbial community (Ma et al., 2024).

While progress has been made towards achieving partial nitrification (Cao et al., 2017; Wang et al., 2022b), the inability to suppress NOB in mainstream partial nitrification-anammox (PNA) is a roadblock to good nitrogen-removal efficiency (Cao et al., 2023; Ji et al., 2020). Partial denitrification has been proposed as a promising alternative to partial nitrification, particularly for low-ammonium municipal wastewater (Ma et al., 2017). In partial denitrification-anammox (PDA), 51 % of the influent NH_4^+ was oxidized to NO_3^-, which was then partially reduced to the NO_2^- needed to oxidize the remaining NH_4^+ by anammox (Ma et al., 2017). Partial denitrification also is effective for the combined treatment of industrial wastewater containing NO_3^- and municipal wastewater containing ammonium (Du et al., 2019).

While information on the impact of N_2H_4 on partial denitrification is absent, NH_2OH is known to inhibit NO_2^- reduction in denitrification. A recent study by Zhang et al. reported that exposure to 5——50 mg N/L of NH_2OH at pH = 9 led to more NO_2^- accumulation by denitrifiers during batch assays (Zhang et al., 2020a). Furthermore, they indicated that NH_2OH at > 0.5 mg N/L inhibited the activity of nitrite reductase due to the substantial suppression of electron transfer to nitrite reductase via cytochrome *c*(Zhang et al., 2022c). Given the strong reducing property of N_2H_4 and its possible analogy with NH_2OH, it is hypothesized that N_2H_4, released from anammox, will increase the accumulation of NO_2^- in partial denitrification and lead to the accumulation of NO_2^- needed for anammox.

The objective of this study was to elucidate the role of N_2H_4 in influencing partial denitrification by examining the connections between reactor performance and microbial ecology. First, the impacts of different concentrations of N_2H_4 on partial denitrification were analyzed, using NO_3^- or NO_2^- as the electron acceptor and acetate as the electron donor in short-term batch experiments. Second, the long-term performance of partial denitrification was evaluated by exposing denitrifiers to three N_2H_4 concentration (0, 0.5, and 1 mg N/L) at influent COD/N ratios of 2.5 or 3 g COD/g N. The COD/N ratios were set at typical values used for partial denitrification in practical applications (Du et al., 2016; Gong et al., 2013); a lower COD/N ratio led to the accumulation of NO_2^- in the effluent, while a higher COD/N ratio led to reduction of NO_2^- to N_2. Finally, the regulatory mechanism of N_2H_4 in partial denitrification was identified through DNA sequencing and bioinformatics analyses.

2. Materials and methods

2.1. Batch experiments

Batch experiments were carried out in sealed brown flasks having a liquid volume of 100 mL (**see supplementary materials**). The biomass was collected from the sequencing batch reactors (SBRs) at the end of Stage I of the long-term experiments (described below), when both SBRs exhibited good partial denitrification. The SBR biomass was washed twice with distilled water to remove residual substrate and then distributed equally into each flask to give a volatile suspended solids (VSS) concentration of ~ 2 g/L. Two sets of batch assays were conducted using six different N_2H_4 inputs (0, 0.5, 1, 2.5, 5, or 10 mg N/L). The electron acceptor of the two sets of batch assays was either NO_3^- or NO_2^-.

The initial NO_3^- or NO_2^- concentration of each batch experiment was set at 60 mg N/L by adding $NaNO_3$ or $NaNO_2$. Trace elements and minerals were added according to previous study (Zhou et al., 2022). The synthetic wastewater was purged with high-purity N_2 gas for 10 min to reduce dissolved O_2 to below 0.2 mg/L. The COD/N ratio was set at ~ 3.0 g COD/g N, which provided more COD than need to reduce all the NO_3^- or NO_2^- to N_2; residual COD was 60——80 mg/L at the end of each batch experiment. The batch reactions were carried out on an orbital shaker (150 rpm, at 30 °C) for two hours. Water samples were collected every 10 min using a disposable syringe. In addition, the interaction of cytochrome *c* (*cyt c*) with N_2H_4 in anaerobic conditions was explored with Ultraviolet/Visible (UV–vis) spectroscopy according to previous study (Zhang et al., 2022c).

2.2. Long-term bioreactor setup and operation

Long-term experiments were conducted using two laboratory-scale sequencing batch reactors (SBRs, **see supplementary materials**) with a volume of 3 L and equipped with a mechanical stirrer (150 rpm) for mixing. The reactors were sealed, and produced N_2 gas exited via a

Table 1
Operational conditions of two SBRs in the different phases.

Stage	Duration (d)	Inf. NO_3^--N (mg/L)	Inf. COD (mg/L)	Inf. N_2H_4-N (mg/L)
I	1–27	60	180 in P1 and P2	0
II-1	28–44	60	180 in P1 and P2	0.5
II-2	45–59	60	180 in P1 and P2	1
III	60–70	60	180 in P1 and P2	0
IV-1	71–82	60	180 in P1 and 150 in P2	0.5
IV-2	83–96	60	180 in P1 and 150 in P2	1
V	97–108	60	180 in P1 and 150 in P2	0

Note: The drainage ratio was 50% for each SBR cycle.

buffer bottle. Feeding was via Braid-Reinforced Polyurethane Tubing and through a peristaltic pump (LongerPump BT100-3 J).

Each SBR was inoculated with 3.0 g VSS/L of activated sludge sourced from a full-scale municipal wastewater treatment plant in Shanghai (China). For each SBR, the temperature was maintained at 30 ± 1℃, the hydraulic retention time (HRT) was 4 h, the reaction time was 3 h, the settling time was 0.5 h, the drainage ratio was fixed at 50 %, and the solids retention times (SRT) was 12 days.

Operation was divided into five stages based on the dose of N_2H_4 and influent COD concentration, as summarized in Table 1. The N_2H_4 solution was prepared from hydrazine hydrochloride (N_2H_4-HCl) and was added separately at the start of each cycle. The synthetic wastewater contained NO_3^- at 60 mg N/L and acetate at 150 or 180 mg COD/L (giving COD/N ratios of 2.5 or 3 g COD/g N), along with trace elements and mineral medium (Zhou et al., 2022). The pH of influent was set at 7.0–7.5 using 1 M HCl or 1 M NaOH. Effluent samples of two reactors were collected daily for chemical analysis.

2.3. Chemical analyses

All liquid samples were immediately filtered through a 0.45-μm membrane filter. The filtered samples were assayed for NH_4^+-N, NO_2^--N, NO_3^--N, SS, and VSS according to *Standard Methods* (APHA, 1985). N_2H_4 was determined using the spectrophotometric method (458 nm) based on its reaction with p-dimethylbenzaldehyde under acidic conditions (Watt and Chrisp, 1952). Total nitrogen (TN) and total organic carbon (TOC) were measured with a Shimadzu TOC-L; dissolved organic nitrogen (DON) was equal to TN minus total inorganic nitrogen (TIN: the sum of NH_4^+-N, NO_2^--N, and NO_3^--N). Soluble COD was analyzed using digestion and spectrophotometric analysis (HACH Model DR 3900).

Effluent samples in Stage IV and V were collected for EEM fluorescence spectroscopy obtained with a Hitachi F-7000 fluorescence spectrophotometer (Hitachi, Japan). The excitation and emission wavelengths ranged from 200 to 550 nm at intervals of 5 nm and at a scan rate of 12000 nm/min. Extracellular polymeric substances (EPS) of the biomass from different stages was extracted and analyzed using the folin-phenol method (for protein) and anthrone method (for polysaccharides) (Du et al., 2023; Zhang et al., 2022a).

2.4. Calculation of COD utilized for biosynthesis

During the long-term experiments, collecting gas from the reactors at the end of each stage and determined the gas composition using an Agilent 7820A gas chromatograph (Agilent, USA). N_2O, NO, and NO_2 had negligible concentrations. Therefore, in the NO_2^- reduction process, NO_2^- was fully reduced to N_2. COD was supplied in the form of acetate (1.07 g COD/g acetate). Complete reduction of NO_3^- to N_2 requires a minimum of 2.86 g COD/g N. Partial reduction of NO_3^- to NO_2^- requires a minimum 1.14 g COD/g N, which means that reduction of NO_2^- to N_2 requires at least 1.72 g COD/g N. Thus, the minimum COD consumed for N-reduction was calculated according Eq. (1):

$$\text{COD utilized for } N-\textit{reduction} = (NO_3^-t0 - NO_3^-\text{eff}) \times 2.86 + (NO_2^-t0 - NO_2^-\text{eff}) \times 1.72 \quad (1)$$

where the NO_{3t0}^- and NO_{2t0}^- are the concentration of NO_3^--N and NO_2^--N at the initiation of a cycle, and NO_{3eff}^- and NO_{2eff}^- are the concentrations of NO_3^--N and NO_2^--N at the end of a SBR cycle. NO_{3t0}^- includes the influent NO_3^- and the residual NO_3^- from the previous SBR cycle, while NO_{2t0}^- is from the residual NO_2^- from the previous cycle. The drainage ratio of SBRs was 50 %.

COD also was incorporated into biomass, and that COD consumption could be computed by difference from the COD removal and the acceptor reductions over a cycle. Therefore, calculating the COD utilized for net biosynthesis from Eq. (2):

$$\textit{COD} \text{ utilized } \textit{forbiosynthesis} = \textit{COD}_{\text{inf}} - \textit{COD}_{\text{eff}} - \textit{COD} \text{ utilized } \textit{for} \text{ N - reduction} \quad (2)$$

where the COD_{inf} and COD_{eff} are the concentration of COD at the start and end of the SBR cycle. In this study, the computed COD uptake for biosynthesis ranged from 5 % to 25 % of the COD consumption for acceptor reduction. These ratios led to the COD biosynthesis values reported in Fig. 2.

2.5. DNA sequencing and bioinformatics analyses

Samples of biomass at the end of Stages I, II-1, II-2, III, IV-1, IV-2, and V were taken for DNA sequencing and bioinformatics analyses. The microbial community was characterized using 16S rDNA sequencing with the primer pair 338F–806R targeting the V3-V4 region according to previous study (Zhou et al., 2022). The biomass samples obtained from the inoculum, Stage IV-2, and Stage V were also analyzed by metagenomic sequencing using the Illumina HiSeq 2500 platform (Majorbio, China) (Dai et al., 2024; Zhou et al., 2024). Taxonomic annotations of the microbial community were performed against the NCBI-NR database using representative sequences from the nonredundant gene catalog. Functional annotation was done using the KEGG database and the DIAMOND algorithm with an e-value cutoff of 1×10^{-5}. Gene abundance was normalized by Reads Per Kilobase Per Million mapped reads (RPKM). All data from DNA-samples sequencing were deposited at the National Center for Biotechnology Information (NCBI)/Sequence Read Archive (SRA) under project PRJNA1131173.

3. Results and discussion

3.1. Effects of N_2H_4 on denitrification in batch experiments

Fig. 1 shows the activity of the denitrifying biomass when exposed to a range of N_2H_4 additions with NO_3^- or NO_2^- as the electron acceptor in the short-term batch experiments. When NO_3^- was the electron acceptor and the initial COD/NO_3^- ratio was 3 g COD/g N, all N_2H_4 concentrations led to a similar, slightly slowed rate of NO_3^- reduction to NO_2^- over the first ~ 30 min (Fig. 1**a**): The best-fit value of the zero-order rate coefficient (k) for the decline in the C/C_0 ratio had a small range —- 1.67 ± 0.01 h^{-1} – for all N_2H_4 concentrations. For NO_2^- in the NO_3^- experiments (Fig. 1**b**), N_2H_4 concentrations ≥ 5 mg/L, caused the NO_2^--N concentration to plateau at about 90 % of the starting NO_3^--N concentration, while N_2H_4 concentrations of 0.5 – 2.5 mg/L slightly slowed the NO_2^--loss rate. When NO_2^- was the electron acceptor (Fig. 1**c**), the rate of NO_2^- reduction was significantly and systematically decreased with increasing of N_2H_4 concentration. The fitted lines in Fig. 1**c** show that the C/C_0 zero-order k values for NO_2^- reduction significantly decreased —- from 0.51 to 0.27 h^{-1} —- when the N_2H_4 concentration increased from 0 to 10 mg N/L. Moreover, in each batch experiment, the concentration difference of N_2H_4 was less than 10 % from start to finish.

Because the batch experiments lasted only 120 min, changes in the rate of consumption of NO_2^- can be attributed to differences in the activity of denitrifying and electron transport enzymes, not to a shift in community structure. During denitrification, the nitrite reductase

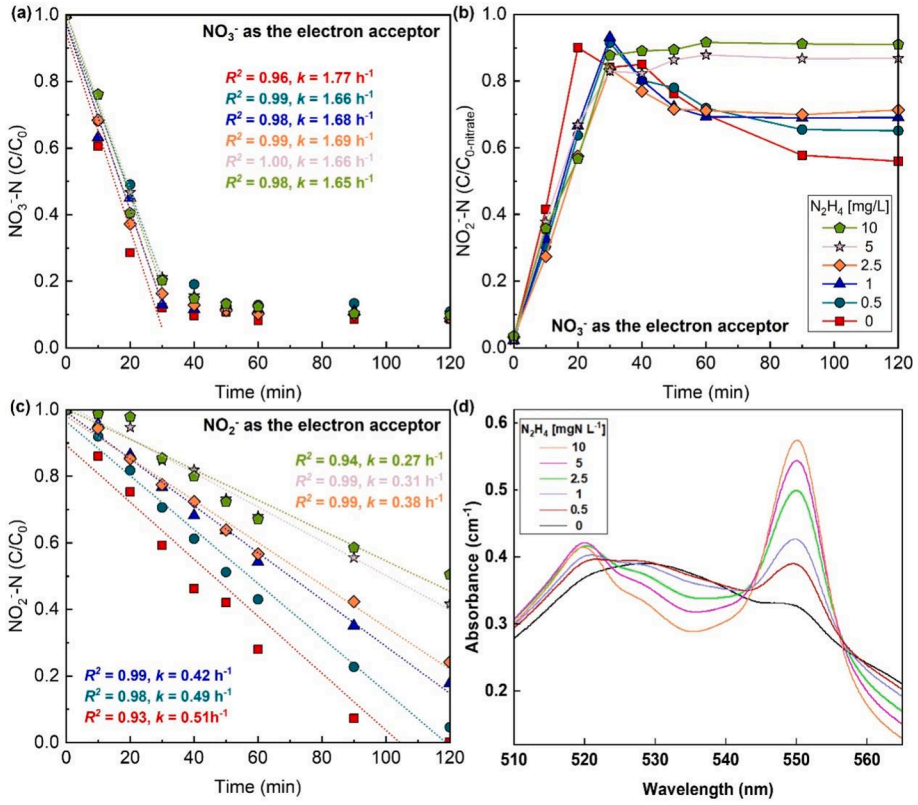

Fig. 1. Fate of NO_3^- (a) and NO_2^- (b) when NO_3^- was the electron acceptor, and fate of NO_2^- (c) when NO_2^- was the electron acceptor, for different dosages of N_2H_4. The initial COD/N ratio was 3 g COD/g N and the initial NO_3^- or NO_2^- concentration was 60 mg N/L. The lines and equations are best-fit linear regressions for the zero-order portions of the C/C_0 data in (a) and (c). (d) Interaction of periplasmic cytochrome *c* with different dosage of N_2H_4, assayed by UV–vis spectrophotometer; peaks around 410 nm are not shown.

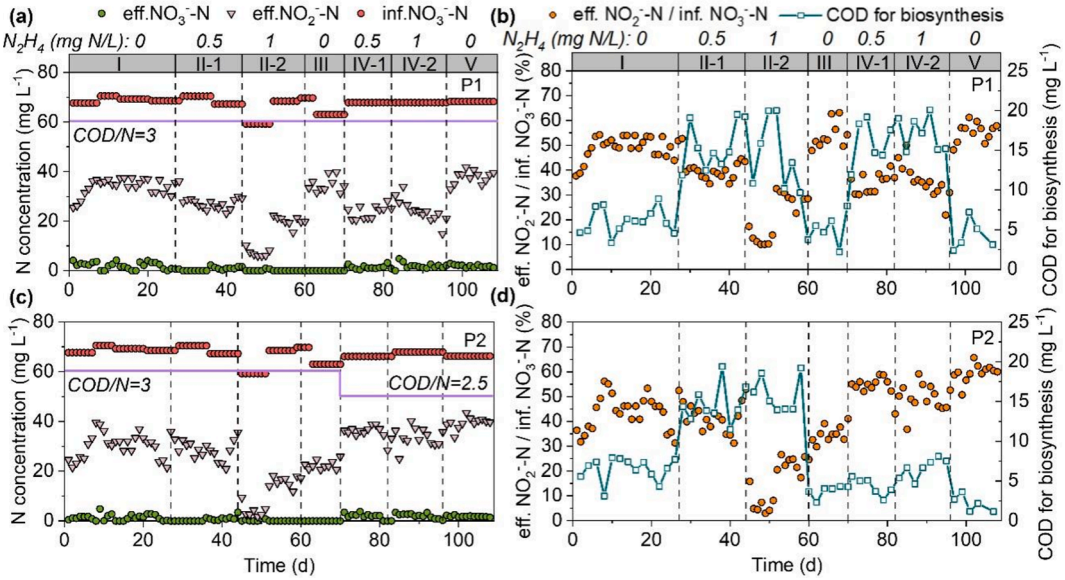

Fig. 2. Long-term performance of two denitrifying reactors (P1 and P2) treated with different input concentrations of N_2H_4 (a, c); and effluent ratio of NO_2^--N / influent NO_3^--N and COD used for biosynthesis (b, d).

receives electrons from soluble *cyt c*, which might be susceptible to N_2H_4 inhibition due to the reaction of N_2H_4 with metal ions located in the active site (Brown et al., 2020; Zhang et al., 2022c). Fig. 1**d** shows that the addition of N_2H_4 caused the *cyt c* peak (527 nm) to shift to two peaks (520 and 550 nm) (Zhang et al., 2022c). This supports that N_2H_4 may interact with *cyt c*, impairing its function and inhibiting electron transport from *cyt c* to nitrite reductase, thereby slowing NO_2^- reduction.

3.2. Long-term performance of the denitrifying reactors with N_2H_4 addition

3.2.1. N_2H_4 inhibited nitrite accumulation

Fig. 2**a and 2c** show the influent and effluent concentrations of NO_3^- and NO_2^- in the long-term P1 and P2 reactors. Fig. 2**b and 2d** summarize the ratio of effluent NO_2^--N / influent NO_3^--N and the concentration of COD used for biosynthesis in the two reactors.

For Stages I to III, the two SBR reactors were operated with the same conditions, including a COD/N ratio of 3 g COD/ g NO_3^--N. Without N_2H_4 addition, NO_2^- accumulated to approximately 50 % of input NO_3^- (Stage I). Once N_2H_4 was added to the SBRs in Stage II, NO_2^- accumulation decreased, and the decline grew to as low as 5 – 10 % as N_2H_4 addition was increased from 0.5 to 1 mg N/L (Stage II-2). However, NO_2^- accumulation returned to ~ 50 % after the N_2H_4 was removed in Stage III.

In Stages IV and V, the P2 reactor was shifted to a COD/N ratio of 2.5 g COD/g N. When N_2H_4 was reintroduced to the P1 reactor in Stage IV, the NO_2^- accumulation performance decreased again, although not as severely as in Stage II, and the ratio was slightly greater in Stage V. In contrast, the P2 reactor achieved greater NO_2^- accumulation, up to 60 %, in Stage IV, but removing N_2H_4 in Stage V led to ratios slightly larger than 60 %. These results document that, in long-term denitrification, the presence of N_2H_4 led to faster NO_2^- reduction at the COD/N ratio of 3 g COD/g N than at 2.5 g COD/g N. These findings were inconsistent with the results of the batch experiments (Fig. 1), in which more N_2H_4 slowed NO_2^- reduction.

COD utilized for biosynthesis (Fig. 2**b and 2d**) increased with N_2H_4 introduction in Stage II and IV for both reactors. N_2H_4 also increased overall COD utilization as NO_2^- reduction increased (**see supplementary materials**), and it does not directly react with NO_2^- (Ma et al., 2018, 2024).

3.2.2. N_2H_4 increased DON release

Fig. 3**a** shows the effluent concentrations of DON during the entire operation of the two reactors. Fig. 3**b – 3d** present the three-dimensional EEM spectra of dissolved organic matter in effluent collected from Stages IV and V in both reactors.

The addition of N_2H_4 significantly increased DON in the effluent of Stages II and IV in both reactors. However, this enhancement was reversed when N_2H_4 was removed in Stage III and V. Furthermore, effluent DON was significantly lower in reactor P2 when its influent COD/N ratio of 2.5 in stage IV and V, compared to 3 g COD/g N for P1. These findings reveal that N_2H_4 and a higher influent COD/N ratio promoting the generation of microorganism-derived DON.

Three peaks were identified in the three-dimensional EEM spectra of effluent samples: Peak A was a protein-like substance (Ex/Em: 275 nm/342 nm), while peaks B and C were humic-like substance (Ex/Em: 325 nm/400 nm and Ex/Em: 250 nm/435 nm) fluorophores (Dai et al., 2024; Jia et al., 2017). Regardless of whether the influent COD/N ratio was 3 or 2.5 g COD/g N (Fig. 3**b and 3c**), the addition of N_2H_4 significantly enhanced the fluorescence intensities of the three peaks in the effluent compared to the stages without N_2H_4 addition (Fig. 3**d**). Furthermore, under N_2H_4 addition conditions, the fluorescence peaks were consistently higher at a COD/N ratio of 3 compared to 2.5. The strongest impact was for protein-like substances (Peak A). These trends reinforce Fig. 3**a** by indicating that N_2H_4 introduction and a higher influent COD/N ratio promoted the release of more soluble microbial products, especially protein-like substances.

3.3. Microbial community composition and interaction

Fig. 4 illustrates the relative abundances of the top 20 bacterial genera in both reactors for Stages I to V. In Stage I, without N_2H_4, the

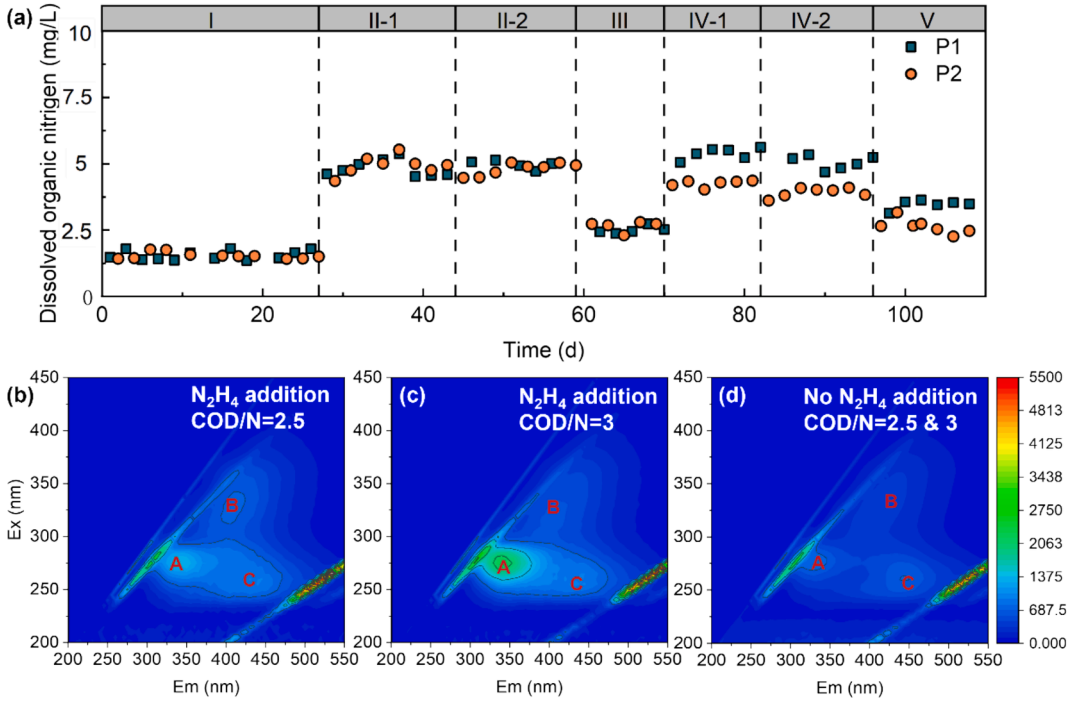

Fig. 3. (a) Effluent dissolved organic nitrogen in two denitrifying reactors (P1, P2). (b) Three-dimensional EEM spectra of dissolved organic matter in effluent collected from Stages with N_2H_4 addition where the influent COD/N ratio was 2.5 g COD/g N (b, Stage IV in P2) and 3 g COD/g N (d, Stage IV in P1); Stages without N_2H_4 addition (c, Stage V in P1 and P2).

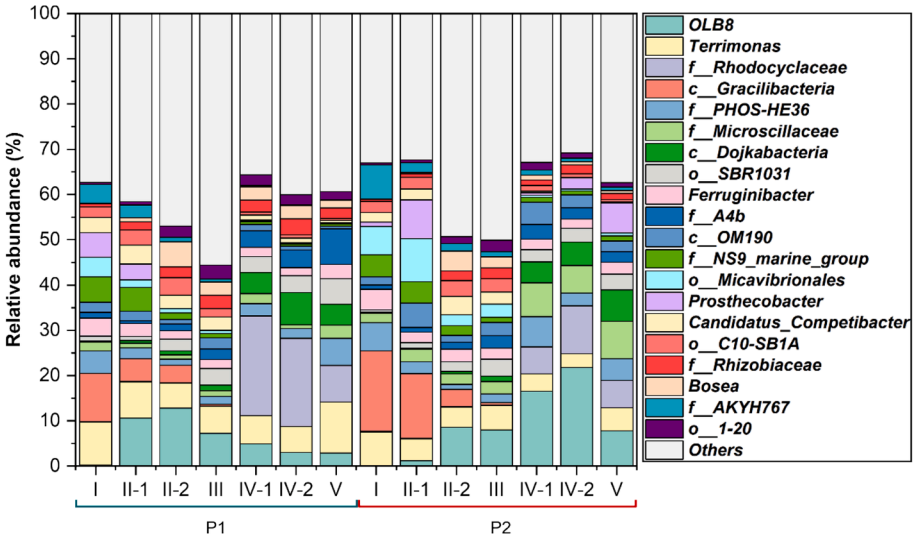

Fig. 4. Relative abundances at the genus level for the microbial communities in P1 and P2 reactors. The difference between the noted percentage abundances and 100% are due to other genera have relative abundance less than 2%.

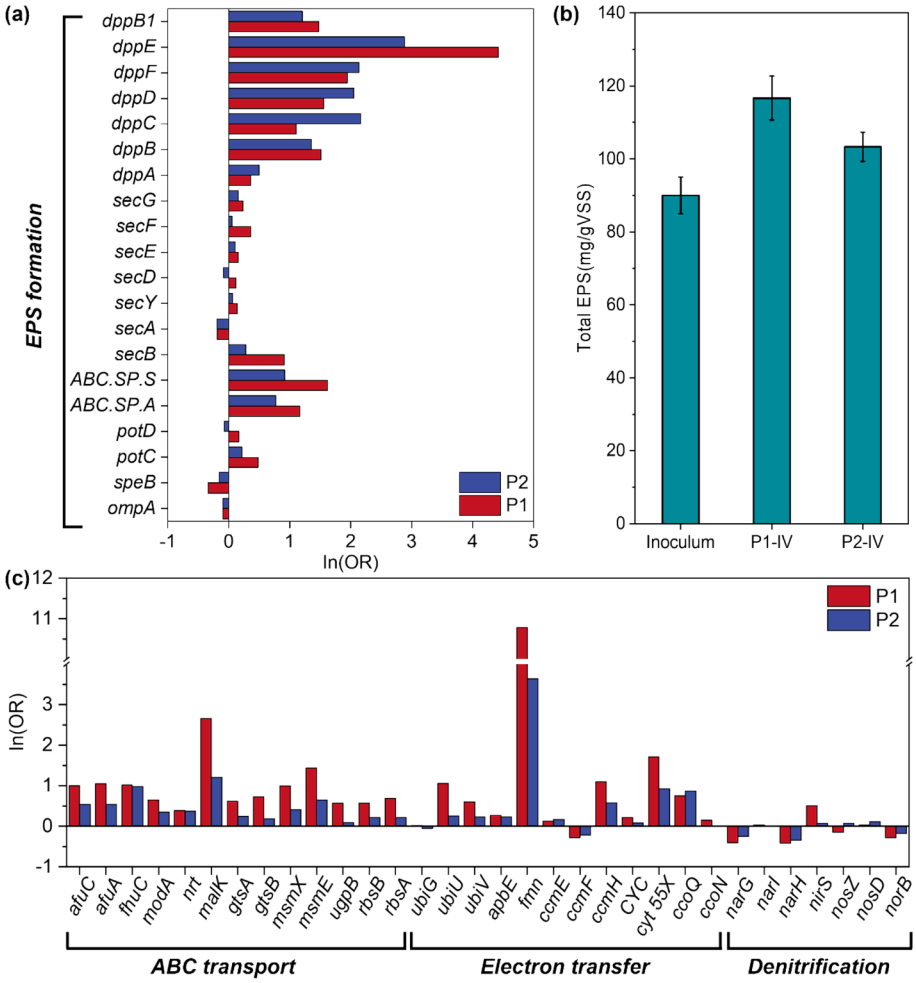

Fig. 5. Odds ratios of average functional genes associated with EPS formation (a) and of carbon, NO_3^-, and metal ABC transporters, electron transport proteins, and denitrification enzymes (c) in Stage IV-2 compared to Stage I. (b) Influence of N_2H_4 addition on the total content of EPS. COD/N ratio = 3 and 2.5 g COD/g N in P1 and P2 respectively.

bacteria were mainly *Terrimonas* and *c_Gracilibacteria*, which are denitrifying bacteria enriched in partial denitrification processes (Cao et al., 2022; Zhang et al., 2021). The dominant bacteria changed to *OLB8* and *f_Rhodocyclaceae* after introduction of N_2H_4 in Stage II, but these two genera again decreased without N_2H_4 addition (Stage III). *OLB8* can oxidize organic matter and synthetize polysaccharides while removing nitrogen and phosphorus simultaneously (Chini et al., 2020). *OLB8* is an incomplete denitrifying bacterium, which means that a high COD/N ratio did not benefit its growth (Hou et al., 2023), a factor that might be related to its higher abundance in P2 reactor when the influent COD/N ratio of 2.5 g COD/g N in Stage V. The genus *f_Rhodocyclaceae* can use a variety of organic substrates to reduce NO_3^- to N_2, and it also has been linked to phosphorus removal (Chen et al., 2024; Li et al., 2023). *OLB8* and *f_Rhodocyclaceae* have capabilities to store intracellular polymers (Chen et al., 2024; Wang et al., 2024a), and it is possible that addition of N_2H_4 promoted the formation of intracellular polymers (glycogen, polyphosphate, and polyhydroxyalkanoate (PHA)) when electron acceptors were in a limited supply (Zhang et al., 2022c). It is possible that intracellular polymers could have been electron donors that helped drive endogenous reduction of NO_2^-(Wang et al., 2016; Zhang et al., 2020b).

3.4. Effect of N_2H_4 on key functional genes

Using odds ratios of average functional genes abundance in Stage IV-2 compared to Stage I, Fig. 5 summarizes the presence of functional genes involved in EPS formation, substrate uptake, and electron transport in P1 and P2. Key genes associated with the main proteins relevant to EPS formation in denitrifying bacteria (*ompA*, *speB*, *pot*, *ABC.SP*, sec, and *ddp*) were greatly increased in the presence of N_2H_4 (Fig. 5**a**). Specifically, genes associated with peptide transporters (*dpp*) were involved in regulating bacterial EPS formation and quorum sensing (Wang et al., 2022a; Wu et al., 2022), exhibiting significant increasing, and enhancing EPS formation through quorum sensing. Consistent with the increase in genes related to EPS formation is that N_2H_4 promoted EPS production by 15——30 % (Fig. 5**b**).

The ATP-binding cassette (ABC) plays a crucial role in transporting substrates into the cells (Schneider, 2001). The abundance of ABC transporter genes, which are responsible for iron transport (*afu*), N transport (*nrt*), and organic-substrate transport (*malK*, *gts*, *msm*, *ugpB*, *rbs*), were significantly increased with N_2H_4 introduction (Fig. 5**c**). Following substrate uptake and oxidation, NO_3^- reduction involves electron being transferred from NADH to N-reductases via complex I, the quinone pool, complex III, and *cyt c* (Chen and Strous, 2013). In particular, genes involved in electron transfer were increased by N_2H_4: ubiquinone biosynthesis (*ubi*), riboflavin-binding (*apbE*, *fmn*), and *cyt c* (*ccm*, *CYC*, *cyt 55X*, *coo*) (Fig. 5**c**), supporting an enhancement of electron transport and more *cyt c* synthesis. However, most genes related to N-reduction were diminished, although *nirS,* responsible for NO_2^- reduction, increased. Therefore, the introduction of N_2H_4 may have led to more electron transfer to the nitrite reductase, resulting in faster NO_2^- reduction and poorer NO_2^- accumulation (Chen and Strous, 2013; Wang et al., 2024b).

All the functional genes, as well as EPS production, were more strongly influenced by N_2H_4 in the P1 reactor (influent COD/N ratio = 3 g COD/g N) compared to P2 reactor (influent COD/N ratio = 2.5 g COD/g N). N_2H_4 seemed to have promoted the uptake and utilization of the organic substrate and corollary NO_2^- reduction, which was amplified by a higher influent COD/N ratio.

3.5. Proposed mechanism

Fig. 6 is a schematic summarizing how N_2H_4 influenced partial

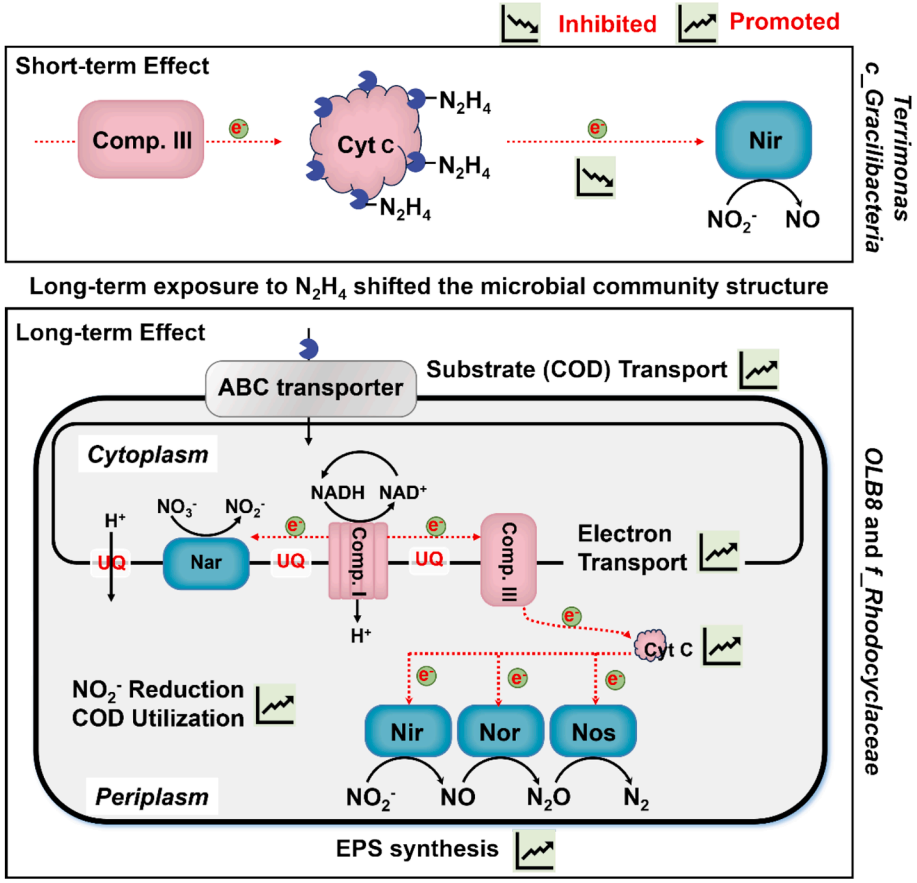

Fig. 6. Proposed regulation mechanisms of N_2H_4 involved in NO_2^- production and reduction during partial denitrification.

denitrification. In the short-term batch experiments, N_2H_4 may interact with *cyt c*, which slowed electron transfer, including to NO_2^- reductase. However, long-term exposure to N_2H_4 led to a change in the microbial community, with *OLB8*, *Thauera*, and *f_Rhodocyclaceae* becoming significantly enriched. Genes for the ABC transporter and EPS synthesis were greatly enhanced, and this resulted in the community's increased ability of transport and utilize the organic substrates via more complete denitrification (**see supplementary materials**). Although the function of *cyt c* is impaired by N_2H_4, the community's denitrifiers counteracted that inhibitory effect by synthesizing more *cyt c* and promoting the reduction of NO_2^-.

4. Conclusions

N_2H_4 (0.5–10 mg/L) induced short-term NO_2^- accumulation in batch experiments, likely by inhibiting the electron transfer from *cyt c* to nitrite reductase. However, at 0.5 or 1.0 mg N/L, this effect did not persist with long-term N_2H_4 input, as most NO_3^- was completely denitrified to N_2. Long-term N_2H_4 exposure altered the microbial community towards genera such as *OLB8*, *Thauera*, and *f_Rhodocyclaceae*, and increased genes related to EPS formation, substrate transport, and *cyt c* synthesis. This promoted EPS production, substrate oxidation, and electron transfer, enhancing NO_2^- reduction. Therefore, long-term N_2H_4 release in partial denitrification-anammox-based wastewater treatment should be avoided.

CRediT authorship contribution statement

Ben Dai: Writing – review & editing, Writing – original draft, Visualization, Resources, Methodology, Investigation, Formal analysis, Data curation, Conceptualization. **Jingzhou Zhou:** Writing – review & editing, Writing – original draft, Visualization. **Zuobin Wang:** Visualization, Validation, Formal analysis. **Yifeng Yang:** Visualization, Investigation, Formal analysis. **Zhenyu Wang:** Investigation. **Junxia He:** Investigation. **Siqing Xia:** Writing – review & editing, Writing – original draft, Supervision, Funding acquisition. **Bruce E. Rittmann:** Writing – review & editing, Writing – original draft, Visualization.

Declaration of competing interest

The authors declare that they have no known competing financial interests or personal relationships that could have appeared to influence the work reported in this paper.

Acknowledgements

This work was supported by National Key Project of Research and Development Plan of China (2021YFC3201300). Dr. Jingzhou Zhou acknowledged the sponsorship of the Shanghai Tongji Gao Tingyao Environmental Science & Technology Development Foundation.

Appendix A. Supplementary data

Supplementary data to this article can be found online at https://doi.org/10.1016/j.biortech.2024.131991.

Data availability

Data will be made available on request.

References

Apha, 1985. Standard methods for the examination of water and wastewater. Apha.
Brown, B.N., Robinson, K.J., Durfee, Q.C., Kekilli, D., Hough, M.A., Andrew, C.R., 2020. Hydroxylamine Complexes of Cytochrome c′: Influence of Heme Iron Redox State on Kinetic and Spectroscopic Properties. Inorg. Chem. 59, 14162–14170. https://doi.org/10.1021/acs.inorgchem.0c01925.
Cao, S., Lan, Y., Peng, Y., Du, R., 2022. Disintegration of Partial Denitrification Granules at High Nitrate Concentration. ACS EST Eng. https://doi.org/10.1021/acsestengg.2c00316.
Cao, S., Koch, K., Duan, H., Wells, G.F., Ye, L., Zhao, Y., Du, R., 2023. In a quest for high-efficiency mainstream partial nitritation-anammox (PN/A) implementation: One-stage or two-stage? Sci. Total Environ. 883, 163540. https://doi.org/10.1016/j.scitotenv.2023.163540.
Cao, Y., van Loosdrecht, M.C.M., Daigger, G.T., 2017. Mainstream partial nitritation–anammox in municipal wastewater treatment: status, bottlenecks, and further studies. Appl. Microbiol. Biotechnol. 101, 1365–1383. https://doi.org/10.1007/s00253-016-8058-7.
Chen, R., Guo, W., Li, L., Wang, H., Wang, B., Hu, X., Ji, B., Zhou, D., Lyu, W., 2024. Aerobic granulation in a continuous-flow simultaneous nitrification, endogenous denitrification, and phosphorus removal system fed with low-strength wastewater: Granulation mechanism and microbial succession. Chem. Eng. J. 487, 150598. https://doi.org/10.1016/j.cej.2024.150598.
Chen, J., Strous, M., 2013. Denitrification and aerobic respiration, hybrid electron transport chains and co-evolution. Biochimica et Biophysica Acta (BBA) - Bioenergetics. The Evolutionary Aspects of Bioenergetic Systems 1827, 136–144. https://doi.org/10.1016/j.bbabio.2012.10.002.
Chini, A., Ester Hollas, C., Chiapetti Bolsan, A., Venturin, B., Bonassa, G., Egidio Cantão, M., Ibelli, M.G., Goldschmidt Antes, F., Kunz, A., 2020. Process performance and anammox community diversity in a deammonification reactor under progressive nitrogen loading rates for swine wastewater treatment. Bioresour. Technol. 311, 123521. https://doi.org/10.1016/j.biortech.2020.123521.
Dai, B., Yang, Y., Wang, Z., Zhou, J., Wang, Z., Zhang, X., Xia, S., 2024. Refractory dissolved organic matters in sludge leachate trigger the combination of anammox and denitratation for advanced nitrogen removal. Water Res. 257, 121678. https://doi.org/10.1016/j.watres.2024.121678.
Dietl, A., Ferousi, C., Maalcke, W.J., Menzel, A., de Vries, S., Keltjens, J.T., Jetten, M.S. M., Kartal, B., Barends, T.R.M., 2015. The inner workings of the hydrazine synthase multiprotein complex. Nature 527, 394–397. https://doi.org/10.1038/nature15517.
Du, R., Peng, Y., Cao, S., Li, B., Wang, S., Niu, M., 2016. Mechanisms and microbial structure of partial denitrification with high nitrite accumulation. Appl. Microbiol. Biotechnol. 100, 2011–2021. https://doi.org/10.1007/s00253-015-7052-9.
Du, R., Cao, S., Peng, Y., Zhang, H., Wang, S., 2019. Combined Partial Denitrification (PD)-Anammox: A method for high nitrate wastewater treatment. Environ. Int. 126, 707–716. https://doi.org/10.1016/j.envint.2019.03.007.
Du, R., Cao, S., Zhang, H., Li, X., Peng, Y., 2020. Flexible Nitrite Supply Alternative for Mainstream Anammox: Advances in Enhancing Process Stability. Environ. Sci. Technol. 54, 6353–6364. https://doi.org/10.1021/acs.est.9b06265.
Du, R., Liu, Q., Li, C., Li, X., Cao, S., Peng, Y., 2023. Spatiotemporal Assembly and Immigration of Heterotrophic and Anammox Bacteria Allow a Robust Synergy for High-Rate Nitrogen Removal. Environ. Sci. Technol. 57, 9075–9085. https://doi.org/10.1021/acs.est.2c08034.
Ganesan, S., Vadivelu, V.M., 2019. Effect of external hydrazine addition on anammox reactor start-up time. Chemosphere 223, 668–674. https://doi.org/10.1016/j.chemosphere.2019.02.104.
Gong, L., Huo, M., Yang, Q., Li, J., Ma, B., Zhu, R., Wang, S., Peng, Y., 2013. Performance of heterotrophic partial denitrification under feast-famine condition of electron donor: A case study using acetate as external carbon source. Bioresour. Technol. 133, 263–269. https://doi.org/10.1016/j.biortech.2012.12.108.
Hou, Z., Dong, W., Wang, H., Zhao, Z., Li, Z., Liu, H., Li, Y., Zeng, Z., Xie, J., Zhang, L., Liu, J., 2023. Response of nitrite accumulation to elevated C/NO– 3-N ratio during partial denitrification process: Insights of extracellular polymeric substance, microbial community and metabolic function. Bioresour. Technol. 384, 129269. https://doi.org/10.1016/j.biortech.2023.129269.
Ji, J., Peng, Y., Wang, B., Li, X., Zhang, Q., 2020. A novel SNPR process for advanced nitrogen and phosphorus removal from mainstream wastewater based on anammox, endogenous partial-denitrification and denitrifying dephosphatation. Water Res. 170, 115363. https://doi.org/10.1016/j.watres.2019.115363.
Jia, F., Yang, Q., Liu, X., Li, X., Li, B., Zhang, L., Peng, Y., 2017. Stratification of Extracellular Polymeric Substances (EPS) for Aggregated Anammox Microorganisms. Environ. Sci. Technol. 51, 3260–3268. https://doi.org/10.1021/acs.est.6b05761.
Jin, R.-C., Yang, G.-F., Yu, J.-J., Zheng, P., 2012. The inhibition of the Anammox process: A review. Chem. Eng. J. 197, 67–79. https://doi.org/10.1016/j.cej.2012.05.014.
Kuypers, M.M.M., Marchant, H.K., Kartal, B., 2018. The microbial nitrogen-cycling network. Nat Rev Microbiol 16, 263–276. https://doi.org/10.1038/nrmicro.2018.9.
Li, X., Li, X., Li, C., Li, N., Zou, P., Gao, X., Cao, Q., 2023. Nitrogen removal performances and metabolic mechanisms of denitrification systems using different volatile fatty acids as external carbon sources. Chem. Eng. J. 474, 145998. https://doi.org/10.1016/j.cej.2023.145998.
Ma, X., Feng, Z.-T., Zhou, J.-M., Sun, Y.-J., Zhang, Q.-Q., 2024. Regulation mechanism of hydrazine and hydroxylamine in nitrogen removal processes: A Comprehensive review. Chemosphere 347, 140670. https://doi.org/10.1016/j.chemosphere.2023.140670.
Ma, B., Qian, W., Yuan, C., Yuan, Z., Peng, Y., 2017. Achieving Mainstream Nitrogen Removal through Coupling Anammox with Denitratation. Environ. Sci. Technol. 51, 8405–8413. https://doi.org/10.1021/acs.est.7b01866.
Ma, J., Yao, H., Yu, H., Zuo, L., Li, H., Ma, J., Xu, Y., Pei, J., Li, X., 2018. Hydrazine addition enhances the nitrogen removal capacity in an anaerobic ammonium oxidation system through accelerating ammonium and nitrite degradation and reducing nitrate production. Chem. Eng. J. 335, 401–408. https://doi.org/10.1016/j.cej.2017.10.132.

Qiao, S., Yin, X., Tian, T., Jin, R., Zhou, J., 2016. Hydrazine production by anammox biomass with NO reversible inhibition effects. Green Chem. 18, 4908–4915. https://doi.org/10.1039/C6GC01261B.

Sari, T., Akgul, D., Mertoglu, B., 2024. Enhancement of hydrazine accumulation in anammox bioreactors. Chemosphere 359, 142293. https://doi.org/10.1016/j.chemosphere.2024.142293.

Schneider, E., 2001. ABC transporters catalyzing carbohydrate uptake. Res. Microbiol. 152, 303–310. https://doi.org/10.1016/S0923-2508(01)01201-3.

Terada, A., Sugawara, S., Hojo, K., Takeuchi, Y., Riya, S., Harper Jr., W.F., Yamamoto, T., Kuroiwa, M., Isobe, K., Katsuyama, C., Suwa, Y., Koba, K., Hosomi, M., 2017. Hybrid Nitrous Oxide Production from a Partial Nitrifying Bioreactor: Hydroxylamine Interactions with Nitrite. Environ. Sci. Technol. 51, 2748–2756. https://doi.org/10.1021/acs.est.6b05521.

Wang, X., Wang, S., Zhao, J., Dai, X., Peng, Y., 2016. Combining simultaneous nitrification-endogenous denitrification and phosphorus removal with post-denitrification for low carbon/nitrogen wastewater treatment. Bioresour. Technol. 220, 17–25. https://doi.org/10.1016/j.biortech.2016.06.132.

Wang, Z., Yu, Q., Zhao, Z., Zhang, Y., 2024b. Ferroheme/Ferriheme Directly Involved in the Synthesis and Decomposition of Hydrazine as an Electron Carrier during Anammox. Environ. Sci. Technol. 58, 10140–10148. https://doi.org/10.1021/acs.est.3c08525.

Wang, M., Zhang, X., Huang, H., Qin, Z., Liu, C., Chen, Y., 2022a. Amino acid configuration affects volatile fatty acid production during proteinaceous waste valorization: chemotaxis, quorum sensing, and metabolism. Environ. Sci. Technol. 56, 8702–8711. https://doi.org/10.1021/acs.est.1c07894.

Wang, X., Zhang, G., Ding, A., Xie, E., Tan, Q., Xing, Y., Wu, H., Tian, Q., Zhang, Y., Zheng, L., 2024a. Distinctive species interaction patterns under high nitrite stress shape inefficient denitrifying phosphorus removal performance. Bioresour. Technol. 394, 130269. https://doi.org/10.1016/j.biortech.2023.130269.

Wang, Z., Zheng, M., Duan, H., Yuan, Z., Hu, S., 2022b. A 20-Year Journey of Partial Nitritation and Anammox (PN/A): from Sidestream toward Mainstream. Environ. Sci. Technol. 56, 7522–7531. https://doi.org/10.1021/acs.est.1c06107.

Watt, G.W., Chrisp, J.D., 1952. Spectrophotometric Method for Determination of Hydrazine. Anal. Chem. 24, 2006–2008. https://doi.org/10.1021/ac60072a044.

Wu, M., Zhang, Z., Zhang, X., Dong, L., Liu, C., Chen, Y., 2022. Propionibacterium freudenreichii-Assisted Approach Reduces N2O Emission and Improves Denitrification via Promoting Substrate Uptake and Metabolism. Environ. Sci. Technol. 56, 16895–16906. https://doi.org/10.1021/acs.est.2c05674.

Xiang, T., Gao, D., 2019. Comparing two hydrazine addition strategies to stabilize mainstream deammonification: Performance and microbial community analysis. Bioresour. Technol. 289, 121710. https://doi.org/10.1016/j.biortech.2019.121710.

Zhang, Q.-Q., Liu, N., Liu, J.-Z., Yu, Y., Ying-Chen, Fu, W.-J., Zhao, J.-Q., Jin, R.-C., 2022. Decoding the response of complete autotrophic nitrogen removal over nitrite (CANON) performance and microbial succession to hydrazine and hydroxylamine: Linking performance to mechanism. Bioresource Technology 363, 127948. https://doi.org/10.1016/j.biortech.2022.127948.

Zhang, M., Gao, J., Liu, Q., Fan, Y., Zhu, C., Liu, Y., He, C., Wu, J., 2021. Nitrite accumulation and microbial behavior by seeding denitrifying phosphorus removal sludge for partial denitrification (PD): The effect of COD/NO3− ratio. Bioresour. Technol. 323, 124524. https://doi.org/10.1016/j.biortech.2020.124524.

Zhang, S., Li, C., Lv, H., Cui, B., Zhou, D., 2024. Anammox activity improved significantly by the cross-fed NO from ammonia-oxidizing bacteria and denitrifying bacteria to anammox bacteria. Water Res. 249, 120986. https://doi.org/10.1016/j.watres.2023.120986.

Zhang, J., Peng, Y., Li, X., Du, R., 2022a. Feasibility of partial-denitrification/ anammox for pharmaceutical wastewater treatment in a hybrid biofilm reactor. Water Res. 208, 117856. https://doi.org/10.1016/j.watres.2021.117856.

Zhang, M., Wang, S., Ji, B., Liu, Y., 2019. Towards mainstream deammonification of municipal wastewater: Partial nitrification-anammox versus partial denitrification-anammox. Sci. Total Environ. 692, 393–401. https://doi.org/10.1016/j.scitotenv.2019.07.293.

Zhang, X., Xia, Y., Wang, C., Li, J., Wu, P., Ma, L., Wang, Y., Wang, Y., Da, F., Liu, W., Xu, L., 2020a. Enhancement of nitrite production via addition of hydroxylamine to partial denitrification (PD) biomass: Functional genes dynamics and enzymatic activities. Bioresour. Technol. 318, 124274. https://doi.org/10.1016/j.biortech.2020.124274.

Zhang, Z., Zhang, Y., Chen, Y., 2020b. Recent advances in partial denitrification in biological nitrogen removal: From enrichment to application. Bioresour. Technol. 298, 122444. https://doi.org/10.1016/j.biortech.2019.122444.

Zhang, Z., Zhang, Y., Shi, Z., Chen, Y., 2022c. Linking Genome-Centric Metagenomics to Kinetic Analysis Reveals the Regulation Mechanism of Hydroxylamine in Nitrite Accumulation of Biological Denitrification. Environ. Sci. Technol. 56, 10317–10328. https://doi.org/10.1021/acs.est.2c01914.

Zhao, J., Zhao, J., Xie, S., Lei, S., 2021. The role of hydroxylamine in promoting conversion from complete nitrification to partial nitrification: NO toxicity inhibition and its characteristics. Bioresour. Technol. 319, 124230. https://doi.org/10.1016/j.biortech.2020.124230.

Zhao, J., Lei, S., Cheng, G., Zhang, J., Shi, B., Xie, S., Zhao, J., 2022. Comparison of inhibitory roles on nitrite-oxidizing bacteria by hydroxylamine and hydrazine during the establishment of partial nitrification. Bioresour. Technol. 355, 127271. https://doi.org/10.1016/j.biortech.2022.127271.

Zhou, J., Wu, C., Pang, S., Yang, L., Yao, M., Li, X., Xia, S., Rittmann, B.E., 2022. Dissimilatory and Cytoplasmic Antimonate Reductions in a Hydrogen-Based Membrane Biofilm Reactor. Environ. Sci. Technol. 56, 14808–14816. https://doi.org/10.1021/acs.est.2c04939.

Zhou, J., Yang, L., Li, X., Dai, B., He, J., Wu, C., Pang, S., Xia, S., Rittmann, B.E., 2024. Biogenic Palladium Improved Perchlorate Reduction during Nitrate Co-Reduction by Diverting Electron Flow in a Hydrogenotrophic Biofilm. Environ. Sci. Technol. https://doi.org/10.1021/acs.est.4c01496.